Traumatic brain injury in children

Konigs, M.

2016

document version
Publisher's PDF, also known as Version of record

CHAPTER 10

THE STRUCTURAL CONNECTOME OF CHILDREN WITH TRAUMATIC BRAIN INJURY

Submitted as:

Königs, M., van Heurn, L. W. E., Bakx, R., Vermeulen, R. J., Goslings, J. C., Poll-The, B. T., van der Wees, M., Catsman-Berrevoets, C. E., Oosterlaan, J., & Pouwels, P. W. J. The structural connectome after traumatic brain injury in children.

ABSTRACT

BACKGROUND

This study aimed to investigate the impact of mild to severe pediatric TBI on differential aspects of the structural connectome.

METHODS

Children aged 8-14 years with trauma control injury (n = 27) were compared to children with mild TBI and risk factors for complicated TBI (mild^{RF+}, n = 20) or moderate/severe TBI (n = 16) at 2.8 years post-injury. Probabilistic tractography on diffusion tensor imaging data was used in combination with graph theory to study structural connectivity. Streamline density (SD) was used to define a network with high probability connections (i.e. connectivity probability network), whereas fractional anisotropy (FA) was used to define a network with high integrity connections (i.e. connectivity integrity network). The minimum spanning tree (i.e. an acyclic subnetwork with maximum connectivity strength) exposed the structural backbone of the constructed networks.

RESULTS

The results revealed that the connectivity probability network primarily captures intrahemispheric connectivity, while the connectivity integrity network has higher sensitivity for interhemispheric connectivity. We found no effects of mild^{RF+} TBI. In contrast, the moderate/severe TBI group showed increased *transitivity* (p = .04, Cohen's d = 0.70) and *assortativity* (p = .04, d = 0.70) in the connectivity probability network, and increased *characteristic path length* in the connectivity probability network (p = .02, d = 0.79), connectivity integrity network (p = .02, d = 0.75) and the backbone of the connectivity integrity network (p = .04, d = 0.66). *Characteristic path length* was related to intelligence and working memory in children with TBI.

CONCLUSIONS

In conclusion, moderate/severe TBI in children alters the structural connectome regarding both high probability connections (increased local clustering and hierarchy) and high integrity connections (reduced integration). Altered structural integration may be implicated in neurocognitive dysfunction after pediatric TBI.

INTRODUCTION

Traumatic brain injury (TBI) is the leading cause of death and acquired disability in children and adolescents (*World Health Organisation*, 2006). The essence of the neuropathology associated with TBI is thought to be represented by widespread axonal injury (Sharp, Scott, & Leech, 2014), threatening the integrity of brain networks that facilitate efficient relay and integration of information throughout the brain (Park & Friston, 2013). Ultimately, children with TBI are at risk of neurocognitive impairments (Babikian & Asarnow, 2009), behavior problems (Li & Liu, 2013) and poor academic attainment (Vu, Babikian, & Asarnow, 2011).

Diffusion tensor imaging (DTI) studies have revealed widespread abnormalities in white matter integrity (i.e. fractional anisotropy; FA) after moderate/severe TBI in children, suggesting the presence of cerebral edema in the acute phase after injury and the presence of axonal degeneration and/or demyelination in the chronic phase (for a meta-analysis, see Roberts, Mathias, & Rose, 2014). Even after mild TBI, acute and subacute white matter abnormalities have been shown in children (Babcock, Yuan, Leach, Nash, & Wade, 2015; Van Beek, Vanderauwera, Ghesquiere, Lagae, & De Smedt, 2015; Yuan, Wade, & Babcock, 2015). Taken together, these findings indicate that white matter is implicated in the neuropathology of TBI across the full range of injury severity.

In recent years, white matter tractography and graph theory have shown to be promising methods to study the impact of neurological disorders on the organization of structural connectivity (i.e. the structural connectome; see Stam, 2014 for a review). Among a handful of studies that used graph theory to assess structural connectivity after TBI, the majority investigated adults with moderate/severe TBI. These studies have used a varying set of network parameters to show that TBI shifts the connectome away from a small world topology (Caeyenberghs, Leemans, De Decker, et al., 2012; Caeyenberghs et al., 2014; Kim et al., 2014), reflecting that the typical equilibrium between structural segregation (i.e. local clustering of connections) and structural integration (i.e. interconnectivity between clusters) shifts towards a lower degree of integration (Rubinov & Sporns, 2010). In adults, complex network measures have shown promising associations with postconcussional symptoms (Dall'Acqua et al., 2016), postural control (Caeyenberghs, Leemans, De Decker, et al., 2012), neurocognitive functioning (Caeyenberghs et al., 2014; Kim et al., 2014) and ratings of disruptive behavior (Kim et al., 2014), highlighting the prognostic potential of network analysis for the outcome of patients with TBI.

The sole study on structural connectivity after pediatric TBI reported results that contrast findings in adults, showing increased small world organization of the structural

connectome during the acute phase of mild TBI (Yuan et al., 2015). In addition to the evident lack of studies into the structural connectome of pediatric TBI patients, the sparse literature into adult TBI shows great methodological variability that further hampers an integrative interpretation of results across studies. For example, studies differ in TBI severity of the patient sample (i.e. mild, moderate, severe or moderate/severe), the recovery phase of interest (i.e. acute, subacute or chronic phase) and the method chosen to reconstruct white matter tracts (e.g. deterministic *vs.* probabilistic tractography; see Qi et al., 2015 for a review). Another crucial difference between studies is the metric chosen to define the structural network of interest, such as streamline density (SD, a measure of connectivity probability) or fractional anisotropy (FA, a measure of connectivity integrity). Differential definitions of the structural network are known to influence network measures, although it remains unknown how this influences connectome reconstruction (Qi et al., 2015). Taken together, the current literature indicates that TBI alters structural brain connectivity, while it remains unclear how TBI affects structural connectivity in the developing pediatric brain, and how varying network definitions capture differential aspects of the structural connectome.

This study aims to elucidate the impact of mild to severe pediatric TBI on the structural connectome in relation to neurocognitive and behavioral outcome in the chronic phase of recovery. Based on the available literature on adult TBI, we expect that pediatric TBI will affect the degree of structural integration in the connectome. Furthermore, we will investigate the influence of two commonly used network definitions (SD and FA) on the reconstruction of the connectome. Given relative high FA in the corpus callosum, we expect that the use of FA to define structural connectivity will produce a network with higher sensitivity to interhemispheric connections as compared to the use of SD. Lastly, we will investigate the impact of pediatric TBI on the structural backbone, as defined by the minimum spanning tree (MST). The MST describes a unique and sparse subnetwork in the connectome, consisting of acyclic (i.e. tree-shaped) connections between all brain areas with minimum connectivity cost (i.e. maximum connectivity strength; Stam et al., 2014). The MST has shown its value in research on the backbone of functional networks affected by neurological and psychiatric disorders (Stam et al., 2014), but has not been used in previous studies on TBI. The results of this study will contribute to our understanding of the impact of TBI on neural connectivity and its implications for functional outcome in children.

METHODS

PARTICIPANTS

This study compared a group of 36 children with TBI to a group of 27 children with trauma control (TC) injury not involving the head, in order to control for pre-injury risk factors of traumatic injury (Max, Koele, & Smith Jr., 1998). Data were collected as part of a follow-up on a consecutive cohort that was retrospectively recruited from three university-affiliated level I trauma centers and three rehabilitation centers in the Netherlands (Königs et al., 2015). Inclusion criteria were: (1) age 8-14 years at time of follow-up; (2) proficient in the Dutch language; (3) children in the TBI group were required to have a history of hospital admission with a clinical diagnosis of either: (a) mild TBI (GCS = 15-13, loss of consciousness [LOC] duration ≤ 30 minutes, post-traumatic amnesia [PTA] duration ≤ 1 hour) with at least one of the following risk factors for complicated TBI (mild^{RF+} TBI) according to the European Federation of Neurological Societies' guidelines on mild TBI: impaired consciousness (GCS = 13-14), focal neurological deficits, persistent vomiting (≥3 episodes), post-injury epileptic seizure, progressive headache and abnormal head CT-scan (Vos & Battistin, 2002); or (b) moderate/severe TBI (GCS = 12-3, LOC duration > 30 minutes, PTA duration > 1 hour; Teasdale & Jennett, 1976); and (4) children in the TC group were required to have a history of hospital admission for traumatic injuries below the clavicles (American College of Surgeons, 2004). Exclusion criteria were: (1) previous TBI; (2) visual disorder interfering with neurocognitive testing; or (3) current neurological condition with known effects on neurocognitive functioning, other than TBI, as documented in medical records or reported in a parent-questionnaire on premorbid functioning.

BACKGROUND INFORMATION

Data on gender, age, socio-economic status (SES) and diagnosed psychiatric or learning disorders were collected using a parental questionnaire. SES was defined as the average level of parental education ranging from 1 (no education) to 8 (postdoctoral education; Statistics Netherlands, 2006).

INJURY SEVERITY

Diagnosed injuries, the lowest score on the GCS on the day of admission, presence of the described risk factors for complicated mild TBI (Vos & Battistin, 2002), and length of hospital stay were extracted from medical files, as was information on any executed surgical procedures. Based on this information, children were assigned to the TC group, mild^{RF+} TBI group or moderate/severe TBI group.

MRI ACQUISITION AND PRE-PROCESSING

MRI was performed at an average 2.8 years post-injury (SD = 1.1) on a 3 Tesla whole-body unit (Discovery MR750, GE Healthcare, Milwaukee, Wisconsin) using an 8-channel head-coil. Three-dimensional T1-weighted images were acquired using a fast spoiled gradient-echo sequence (176 slices, acquisition matrix 256 x 256, voxel-size 1 x 1 x 1 mm, TR/TE/TI = 8.2/3.2/450 ms, flip angle 15˚). Furthermore, two-dimensional echo-planar diffusion-tensor images were acquired in 5 volumes without diffusion weighting and 30 volumes with non-collinear diffusion gradients (b-value = 750 s/mm^2) in 47 oblique slices of 2.5 mm thickness covering the whole brain (TR/TE = 5000/74 ms). The acquired in-plane resolution was 2.5 x 2.5 mm, reconstructed to 1 x 1 mm using interpolation. Parallel imaging was applied with an acceleration factor of 2. All processing of MR images was performed using the Functional MRI of the Brain (FMRIB) Software Library (FSL) version 5.0.8 (Jenkinson, Beckmann, Behrens, Woolrich, & Smith, 2012). Pre-processing of diffusion-tensor images, including correction for motion and eddy currents, is described in detail elsewhere (Königs et al., submitted). Subsequent data processing is described below and a visual representation of the data processing pipeline is provided in Figure 1.

PROBABILISTIC TRACTOGRAPHY

We performed probabilistic tractography to infer the structural connectivity between a priori defined regions-of-interest (ROI). The Automated Anatomic Labeling (AAL) atlas (Gong et al., 2009) was used to define neocortical ROIs (*n* = 78), while FIRST (Patenaude, Smith, Kennedy, & Jenkinson, 2011) was used to define subcortical ROIs (*n* = 14: thalamus, caudate nucleus, putamen, globus pallidum, hippocampus, amygdala and accumbens nuclei in both hemispheres). All ROIs (for a complete list, see Supporting Table S1) were registered to subject space and subsequently rimmed to confine tractography from and to the border between grey matter and white matter. For the cortical ROIs, we calculated a rim of two voxels thickness by subtracting an eroded white matter mask from a dilated white matter mask (obtained using FAST; Zhang, Brady, & Smith, 2001). We subsequently multiplied the resulting rim with the AAL atlas in subject space to obtain rim masks of the cortical ROIs. For subcortical ROIs, rim masks were obtained by subtracting twice-eroded masks from subcortical ROI masks. The resulting cortical and subcortical rim masks (*n* = 92) were each used as both seeds and targets for probabilistic tractography. BEDPOSTX (Behrens et al., 2003) was used to model multiple fiber orientations per voxel in the diffusion weighted maps, and finally probabilistic tracking was performed using PROBTRACKX2 in subject space (Behrens et al., 2003). A total of 500 streamlines were generated from each voxel in each seed ROI (using a curvature threshold of 0.2 and step length of 0.5 mm) and streamlines were terminated if they reached one of the target ROIs (*n* = 91). Streamlines with interhemispheric crossings outside the corpus callosum and fornix were discarded.

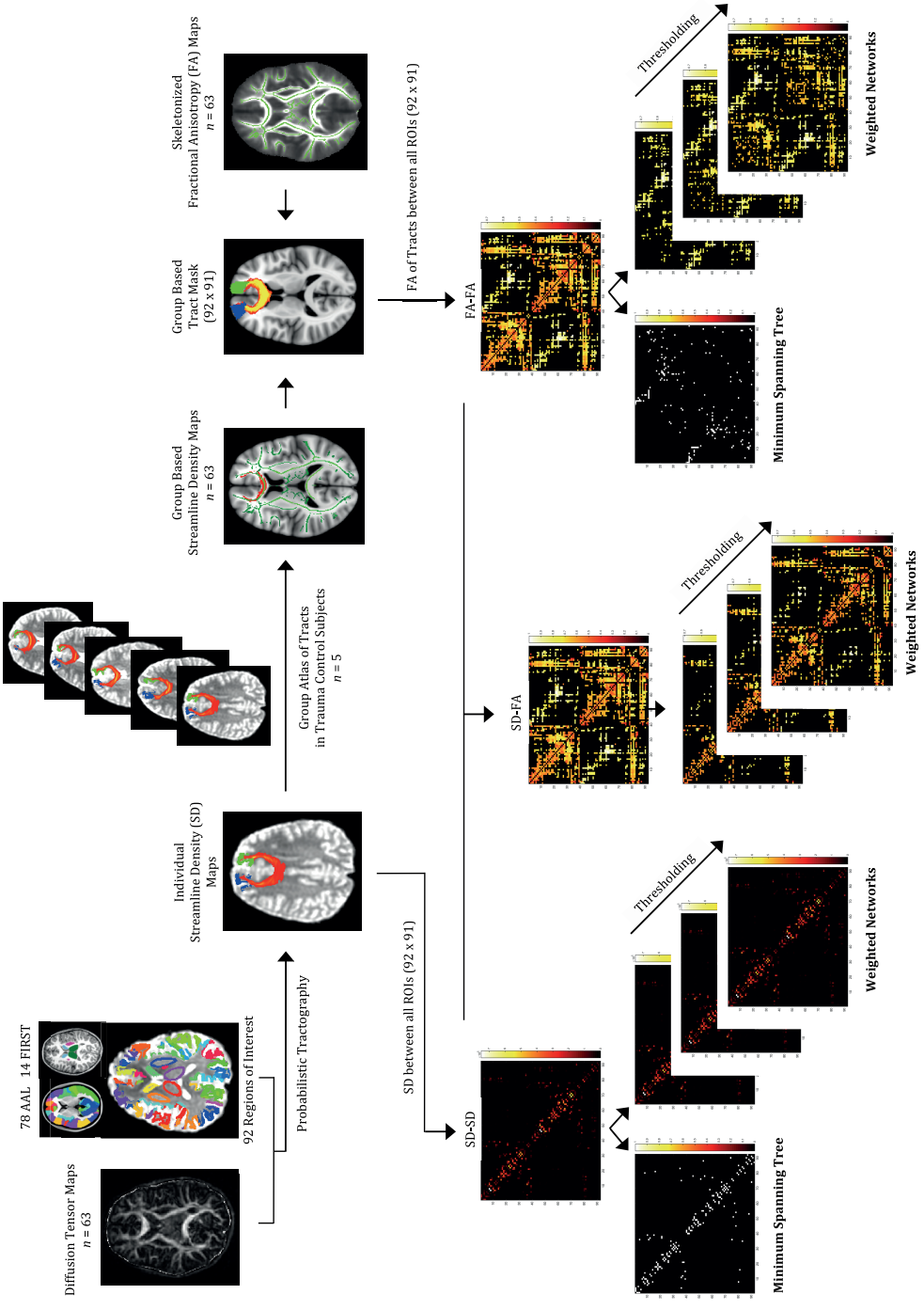

Figure 1. Data processing for the construction of connectivity matrices

Note. Cortical ROIs were derived from the AAL atlas and subcortical ROIs were segmented using FIRST, which were all confined to the border between grey and white matter. These 'rimmed' ROIs were used as both seeds and targets in probabilistic tractography. This produced individual streamline density (SD) maps, from which SD between each seed-target pair was used to define binary SD matrices. SD-SD matrices were additionally weighted for SD. Subsequently, the individual SD maps of five representative trauma control subjects were used to construct an atlas of white matter tracts. The individual SD maps of all seed-target pairs were registered to MNI-152 space, averaged across subjects and subsequently confined to the 5% strongest voxels in order to provide a conservative group-based atlas of tracts between all seed-target pairs. The mask of each tract was superimposed on the skeletonized FA map of each subject (as derived using tract-based spatial statistics) to calculate mean FA in each tract, which was subsequently used to weight SD-FA matrices and to define and weight FA-FA matrices. SD-SD, SD-FA and FA-FA matrices were proportionally thresholded at 10, 15 and 20%, representing networks with the 419, 628 and 837 strongest connections, respectively. Lastly, the minimum spanning tree was used to capture the backbone of the SD-SD and FA-FA matrices. AAL = Automated Anatomical Labeling atlas (Gong et al., 2009); FIRST (Patenaude et al., 2011) refers to a model-based segmentation tool from the Functional MRI of the Brain Software Library (FSL); SD = streamline density; ROIs = regions of interest; FA = fractional anisotropy.

CONNECTIVITY MATRIX CONSTRUCTION

MATRIX TYPES

We used SD and FA to create three types of connectivity matrices for each subject. Visual representations of the corresponding networks are displayed in the left panel of Figure 2 (produced using qgraph; Epskamp, Cramer, Waldorp, Schmittmann, & Borsboom, 2012). We used SD to define connectivity matrices that capture the network with the highest connectivity probability (i.e. the connectivity probability network). These binary SD-defined matrices were subsequently weighted for SD to account for differences in connectivity probability between brain regions (SD-SD matrices), and were also weighted for FA in order to account for differences in connectivity integrity within the connectivity probability network (SD-FA matrices). We also constructed FA-defined matrices in order to capture the network with the highest connectivity integrity (i.e. the connectivity integrity network), which were weighted for FA to account for differences in connectivity integrity between brain regions in this network (FA-FA matrices).

MATRIX WEIGHTS

SD of a given tract was defined by the number of streamlines that connect the involved seed-target pair (ROI X to ROI Y and vice versa), where higher SD corresponds to higher connectivity probability. SD weights were obtained as part of the output from PROBTRACKX2 (see Probabilistic tractography). FA of a given tract was defined by mean FA in a set of streamlines connecting the involved seed-target pair (ROI X to ROI Y and vice versa), where higher FA corresponds to higher connectivity integrity. FA weights were

derived according to a method described by Squarcina, Bertoldo, Ham, Heckemann, & Sharp (2012), which has been found to produce accurate and robust results in patients with TBI (Fagerholm, Hellyer, Scott, Leech, & Sharp, 2015). Using the spatial SD distributions resulting from PROBTRACKX2, a white matter tract atlas was constructed based on a subgroup of five subjects from the TC group that was representative for the total TC group (age: M = 10.6, SD = 1.4, gender: 60% males, SES: M = 6.0, SD = 0.9). For these five subjects, spatial SD distributions connecting each seed-target pair were registered to MNI-152 space and subsequently averaged across the subjects. The resulting group-based spatial SD distributions were then confined to the 5% voxels with the highest SD and binarized to produce a conservative atlas of white matter tract masks. The mask of each tract was superimposed on the skeletonized FA map of each subject (FA > 0.2, constructed using FSL's Diffusion Toolbox) to calculate mean FA across streamlines connecting each seed-target pair within the white matter skeleton, which was subsequently used as weight in the FA-weighted matrices.

MATRIX THRESHOLDING

The weighted SD-SD, SD-FA and FA-FA matrices were proportionally thresholded by selecting the 10%, 15% and 20% strongest connections in the network in order to accounting for the influence of thresholding on network parameters (Qi et al., 2015). The resulting weighted matrices captured a fixed number of 419, 628 and 837 strongest connections in the network (i.e. links), respectively, while the number of nodes (i.e. ROIs that were captured in the network) was not fixed. The weighted connectivity matrices capture a relatively large part of the structural network and are sensitive for diffuse effects on weighted connectivity (Qi et al., 2015).

MINIMUM SPANNING TREE

In addition to the construction of weighted networks, the MST was used to define the backbone of the structural network (see the right panel of Figure 2). The MST is a unique binary subnetwork (assuming that all edge weights are unique) that captures acyclic (i.e. tree-shaped) connections between all ROIs in the network while minimizing network cost (i.e. maximizing the sum of connectivity weights; Stam et al., 2014). In order to capture the backbones of the structural network with the maximum sum of SD weights (i.e. maximum connectivity probability) and FA weight (i.e. maximum connectivity integrity), we calculated MSTs on the *inversely* weighted SD-SD and FA-FA matrices, respectively (Otte et al., 2015). Calculation of the MST on the SD-FA matrices was omitted since the resulting binary graph would be identical to the MST of the FA-FA matrices. Use of the MST eliminates the need for thresholding and has a fixed number of nodes (N = 92) and links (N-1 = 91).

GLOBAL NETWORK PARAMETERS

Graph theory was used to study the properties of the constructed SD-SD, SD-FA and FA-FA networks and their MSTs. Graph theory is an influential method in neural connectivity analysis that describes the organization of a network according to the distribution of links between nodes. An in-depth review of graph theory is provided elsewhere (Rubinov & Sporns, 2010). Graph analysis can be used to describe connectivity at the level of the network using global network parameters. The Brain Connectivity Toolbox (Rubinov & Sporns, 2010) was used to calculate global network parameters for the weighted networks and the MSTs. Global network parameters were transformed to z-scores in order to allow group comparisons on the same scale for all parameters in all of the assessed networks.

We used *characteristic path length*, *transitivity, assortativity* and *modularity* to describe the organization of structural connectivity of the global network. In short, *characteristic path length* is a measure of integration defined by the average shortest distance between nodes, where distance is defined by the average number of links that connect a node to all other nodes. *Transitivity* is a measure of local clustering, defined by the ratio of triangles (i.e. three nodes connected in a closed triangle) to triplets (i.e. three nodes connected in an open triangle), where higher *transitivity* reflects stronger clustering of nodes. *Transitivity* was not calculated for the MSTs, since the MST is an acyclic graph that does not capture triangles in the network. *Modularity* is a measure of clustering at the level of modules, which are subdivisions of the network in groups of nodes with many links to nodes within the group and few links to nodes outside the group. Higher *modularity* refers to a stronger subdivision of the network into modules. *Assortativity* is a measure of hierarchy, defined by the correlation between the *degree* (i.e. number of links attached to a node) of connecting nodes. Consequently, higher (more positive) *assortativity* coefficients describe a stronger tendency of nodes to connect to other nodes with a similar degree. An overview of constructs and variables relating to network analysis is provided in Table 1.

Table 1. Global network parameters as derived using graph analysis

Variable	Description
Connectivity Metrics	
Streamline Density	Streamline density (SD) of a given tract was defined by the number of streamlines that connect the involved seed-target pair (region of interest X to region of interest Y and vice versa), where higher SD corresponds to higher connectivity probability.
Fractional Anisotropy	Fractional anisotropy (FA) of a given tract was defined by mean FA in a set of streamlines connecting the involved seed-target pair (region of interest X to region of interest Y and vice versa), where higher FA corresponds to higher connectivity integrity.
Network Components	
Node	A region of interest that is captured in the network.
Link	A connection between two nodes that is captured in the network.
Link Weight	A metric reflecting the connectivity between two nodes on a scale.
Network Types	
Weighted Network	A network in which links are weighted for a connectivity metric (e.g. SD or FA).
Minimum Spanning Tree (MST)	The minimum spanning tree (MST) is a unique binary subnetwork that connects all nodes in the network in an acyclic (i.e. tree-shaped) fashion while minimizing the network cost (i.e. maximizing the sum of link weights). The MST captures the backbone of the network.
Network Definitions	
SD-SD Network	A network defined by SD and weighted by SD. This approach captures the network with the highest connectivity probability (i.e. the connectivity probability network) and accounts for differences in connectivity probability between nodes.
SD-FA Network	A network defined by SD and weighted by FA. This approach captures the network with the highest connectivity probability (i.e. the connectivity probability network) and accounts for differences in connectivity integrity between nodes.
FA-FA Network	A network defined by FA and weighted by FA. This approach captures the network with the highest connectivity integrity (i.e. the connectivity integrity network) and accounts for differences in connectivity integrity between nodes.
MST of SD-SD	The structural backbone of the connectivity probability network.
MST of FA-FA	The structural backbone of the connectivity integrity network.
Global Network Parameters	
Characteristic Path Length	*Characteristic path length* is a measure of integration defined by the average shortest distance between nodes, where distance is defined by the average number of links that connects a node to all other nodes.
Transitivity	*Transitivity* is a measure of local clustering, defined by the ratio of triangles (i.e. three nodes connected in a closed triangle) to triplets (i.e. three nodes connected in an open triangle). Higher *transitivity* reflects stronger local clustering of nodes in the network.
Modularity	*Modularity* is a measure of clustering at the level of modules, which are subdivisions of the network in groups of nodes with many links to nodes within the group and few links to nodes outside the group. Higher *modularity* refers to a stronger subdivision of the network into modules.
Assortativity	*Assortativity* is a measure of hierarchy, defined by the correlation between the *degree* (i.e. number of links attached to a node) of connecting nodes. Consequently, higher (more positive) assortativity coefficients describe a stronger tendency of nodes to connect to other nodes with a similar degree.

Note. FA = fractional anisotropy; MST = minimum spanning tree; SD = streamline density.

FUNCTIONAL OUTCOME

We used aspects of neurocognitive and behavioral functioning with proven sensitivity for TBI as measures of functional outcome. In a previous study, we already showed that the current mild^{RF+} TBI and moderate/severe TBI groups had lower intelligence, poorer working memory performance, poorer encoding of information in working memory and more internalizing behavior (e.g. symptoms of anxiety and depression) and externalizing behavior problems (e.g. aggression and delinquent behavior) than the TC group (Königs et al., submitted). Consequently, we selected these outcome measures to study the relation between network parameters and functional outcome.

Intelligence was measured by a Wechsler Intelligence Scale (WISC)-III (Wechsler, 2005) short-form estimation of age-standardized full-scale IQ (FSIQ), involving the Vocabulary and Block Design subtests. This short form has high validity and reliability in estimating full FSIQ (Sattler, 2001). Working memory was measured using the age-standardized score on the Digit Span subtest of the WISC-III (Wechsler, 2005). The Rey Auditory Verbal Learning Test (RAVLT) (van den Burg & Kingma, 1999) was used to measure encoding in verbal memory using the age-standardized z-scores on the direct recall condition. Behavioral functioning was measured using parent and teacher ratings of internalizing problems and externalizing problems, obtained using the Child Behavior Checklist and the Teacher Rating Form, respectively (Verhulst & van der Ende, 2013). Age- and gender- standardized T-scores of parents and teacher ratings were averaged to yield composite scores of internalizing and externalizing problems. For clarity reasons, all functional outcome scores were transformed to z-scores where lower values intuitively correspond to poorer neurocognitive performance/less behavior problems. A replication of the previously reported group comparisons on functional outcome measures is provided in the Supporting Information.

PROCEDURE

Of all 123 children that were eligible for the current follow-up (TBI: $n = 67$; TC: $n = 56$), 11 were not reached (TBI: $n = 8$; TC: $n = 3$) and 36 declined participation (TBI: $n = 17$; TC: $n = 19$). Main reasons not to participate were: not interested (TBI: 41%; TC: 32%), objection to MRI (TBI: 0%; TC: 21%) and lack of time (TBI: 24 %; TC: 21%). A total of 12 children were excluded from participation due to dental braces incompatible with MRI (TBI: $n = 2$; TC: $n = 6$), claustrophobia (TBI: $n = 2$; TC: $n = 1$), major brain damage after neurosurgical resection (TBI: $n = 1$; TC: $n = 0$) or no show (TBI: $n = 1$; TC: $n = 0$). The remaining children in the TBI and TC groups (TBI: $n = 36$; TC: $n = 27$) did not differ from their respective cohorts in terms of age, gender and SES (TBI: $ps \geq .28$; TC: $ps \geq .07$), or GCS score (TBI: $p = .68$). The current follow-up took place at an average 2.8 years post-injury.

Written informed consent was provided by parents and children aged > 11 years. Trained examiners administered the neurocognitive tests in a fixed order, while parents filled out questionnaires in a waiting room. Subsequently, children were made familiar with the MRI procedure using a simulation scanner before actual MRI scanning was performed in the VU University Medical Center. The medical ethical committee of the VU University Medical Centre approved this study (NL37226.029.11).

STATISTICAL ANALYSIS

All dependent variables were screened for outliers using box-plots. Modularity data in the weighted SD-SD and SD-FA networks (all thresholds) were subjected to a van der Waerden transformation in order to reduce the influence of outliers (Lehmann & D'Abrera, 2006). To explore group comparability, all groups (TC, mild^{RF+} TBI and moderate/severe TBI) were compared on demographics, injury severity variables and the prevalence of clinical diagnoses of psychiatric or learning disorders, using ANOVA or chi-square tests, where appropriate.

Analyses on network properties were performed in four steps, assessing: (1) the influence of differential network definition and/or weighting on the sensitivity for interhemispheric connectivity in the weighted networks (i.e. SD-SD, SD-FA and FA-FA) and their structural backbones (i.e. MST of SD-SD and MST of FA-FA); (2) the impact of TBI on global network properties of the weighted networks and their structural backbones; and (3) the relations among network parameters with obtained effects of TBI and their associations with functional outcome after pediatric TBI.

Firstly, we compared the influence of various network definitions on the sensitivity of the resulting network for interhemispheric connectivity. Sensitivity for interhemispheric connectivity was defined as the percentage of interhemispheric connections relative to all connections in the network. With regard to the weighted networks (i.e. SD-SD, SD-FA and FA-FA) we calculated the sum of interhemispheric link weights (i.e. SD or FA associated with each link that represented an interhemispheric connection) as a percentage of the sum of link weights in the total network, at each of the matrix thresholds. Since the MSTs are binary networks, we calculated the sum of interhemispheric links as a percentage of the total number of links in the MST. For the weighted networks, we compared the influence of network definition on interhemispheric connectivity using a repeated measure ANOVA on interhemispheric link weight (%), with network definition (SD-SD, SD-FA, FA-FA) and matrix threshold (10%, 15%, 20%) as within-subject variables. If a significant effect of network definition was observed, the influence of matrix threshold on the effect of network definition was also assessed using the interaction effect between network

definition and matrix threshold. With regard to the MSTs, we investigated the influence of network definition on interhemispheric connectivity using a repeated measures ANOVA on interhemispheric links (%), with network definition (MST of SD-SD, MST of FA-FA) as the only within-subject variable (since the MST is independent of matrix thresholding).

Secondly, we assessed the impact of TBI on global connectivity in the SD-SD, SD-FA and FA-FA networks. Global network parameters derived from weighted matrices (*characteristic path length*, *transitivity*, *modularity* and *assortativity*) were compared between groups using repeated measures ANOVAs, with matrix threshold as within-subjects variable (10%, 15% and 20%). Global network parameters derived from MST matrices (*characteristic path length*, *modularity* and *assortativity* derived from the MSTs of the SD-SD and FA-FA networks) were compared between groups using ANOVA.

Thirdly and lastly, we investigated the relations between network parameters that showed a main effect of group in analysis 2, using Pearson correlations in the sample of children with TBI. Likewise, we assessed the relations between these network parameters and the selected measures of neurocognitive and behavioral functioning (see Functional outcome and Supporting Information). The z-scores of network parameters derived from the weighted matrices were averaged across the assessed matrix thresholds before correlations with other variables were calculated.

In all described ANOVAs, we used the linear main effect of group (TC, mild^{RF+} TBI and moderate/severe TBI) to assess the impact of TBI severity on the described dependent variables. For all ANOVAs on weighted matrices with significant main effects of group, the influence of matrix threshold on the effect of group was also reported, assessed using the interaction effect between group and matrix threshold on the relevant dependent variable. All ANOVAs with significant main effects of group were followed by pair-wise comparisons between groups using post-hoc LSD testing. For all statistical analyses, α was set at .05 (two-sided) and effect sizes were expressed in Cohen's *d* (Cohen, 1988).

RESULTS

PATIENT CHARACTERISTICS

Table 2 displays data on demographics, injury-severity variables and prevalence of psychiatric and learning disorders for all groups. There were no group differences on demographic variables (*p*s ≥ .17), except for lower SES in the mild^{RF+} TBI and moderate/severe TBI groups as compared to the TC group (*p*s ≤ .04). With regard to injury-related variables, as expected the moderate/severe TBI group had lower GCS scores than the mild^{RF+} TBI group ($p < .001$), while higher prevalence of neurosurgery and longer hospital stay were observed as compared to both the mild^{RF+} TBI group and TC group (*p*s ≤ .009). As a result of our recruitment strategy, the TC group had higher prevalence of extracranial fractures and orthopedic surgery than both the mild^{RF+} TBI group (*p*s < .001) and the moderate/severe TBI group (*p*s < .001). Last, there were no significant group differences in the prevalence of psychiatric or learning disorders (*p*s > .06).

Table 2. Demographic and injury-related characteristics in TBI and TC groups

	Groups			Contrasts
	TC	Mild RF+ TBI	Moderate/Severe TBI	
n	27	20	16	
Demographics				
Males, n (%)	12 (44)	13 (65)	10 (58)	NS
Age at testing in y	10.2 (1.5)	10.5 (1.8)	9.9 (1.4)	NS
SES	6.3 (1.1)	5.5 (1.3)	5.0 (1.1)	M, MS < TC
Injury-related information				
Age at injury in y	7.5 (2.2)	7.7 (2.3)	6.9 (1.9)	NS
Lowest GCS	-	14.5 (0.7)	8.2 (2.8)	M > MS
Hospital Stay in *d*	2.5 (2.0)	3.5 (2.4)	8.1 (7.3)	MS > TC, M
Time since injury in y	2.7 (1.0)	2.8 (1.1)	3.0 (1.5)	NS
Range	*1.0-4.5*	*0.8-53*	*1.0-6.2*	
Extracranial fracture, n (%)	23 (85)	4 (20)	2 (13)	M, MS < TC
>1 Extracranial fractures, n (%)	3 (11)	1 (5)	0 (0)	NS
Orthopedic surgery, n (%)	22 (82)	2 (10)	0 (0)	M, MS < TC
Neurosurgery, n (%)	0 (0)	0 (0)	4 (25)	MS > TC, M
Diagnosed conditions				
Psychiatric disorder, n (%)	1 (4)	2 (10)	1 (6)	NS
Learning disorder, n (%)	2 (7)	4 (20)	0 (0)	NS

Note. Data reflect mean (standard deviation), unless otherwise indicated. ADHD = attention deficit hyperactivity disorder; d = days; GCS = Glasgow Coma Scale; M = mildRF+ TBI group; MS = moderate/severe TBI group; NS = not significant; RF = risk factor; SES = socio-economic status; TBI = traumatic brain injury; TC = traumatic control; y = years.

NETWORK DEFINITIONS

Confirming qualitative observations (see Figure 2), we found a main effect of network definition on the interhemispheric weight in the weighted networks (see Table 2), indicating that the sensitivity to interhemispheric connectivity varied between the network definitions. More specifically, SD-SD, SD-FA and FA-FA networks had progressively higher interhemispheric weight (*p*s < .001) indicating progressively higher sensitivity for interhemispheric connectivity. The interaction effect between network definition and matrix threshold on interhemispheric weight also was significant, indicating that the effect of network definition on interhemispheric connectivity significantly differed across the assessed matrix thresholds. More specifically, SD-SD and SD-FA networks showed increasing interhemispheric weight with increasing matrix threshold (*ps* < .001), reflecting that a higher matrix threshold was associated with higher sensitivity for interhemispheric connectivity. Conversely, FA-FA networks showed decreasing interhemispheric weight with increasing matrix threshold (*p* < .001), indicating that a higher matrix threshold was associated with lower sensitivity for interhemispheric connectivity.

With regard to the MSTs, a significant effect of network definition on interhemispheric link percentage was found (Table 2). More specifically, the MST of the SD-SD network had lower interhemispheric link weight as compared to the MST of the FA-FA network. In fact, the former primarily captured intrahemispheric connectivity, while the latter primarily captured interhemispheric connectivity. Taken together, these findings indicate that network definition greatly influences the reconstruction of the connectome. Networks as defined and weighted by SD primarily describe intrahemispheric connectivity, while the use of FA to weight and/or define the network increases its sensitivity for interhemispheric connectivity. Lastly, higher matrix thresholds are associated with a reduction in the difference between SD defined and FA defined networks in terms of their sensitivity for interhemispheric connectivity.

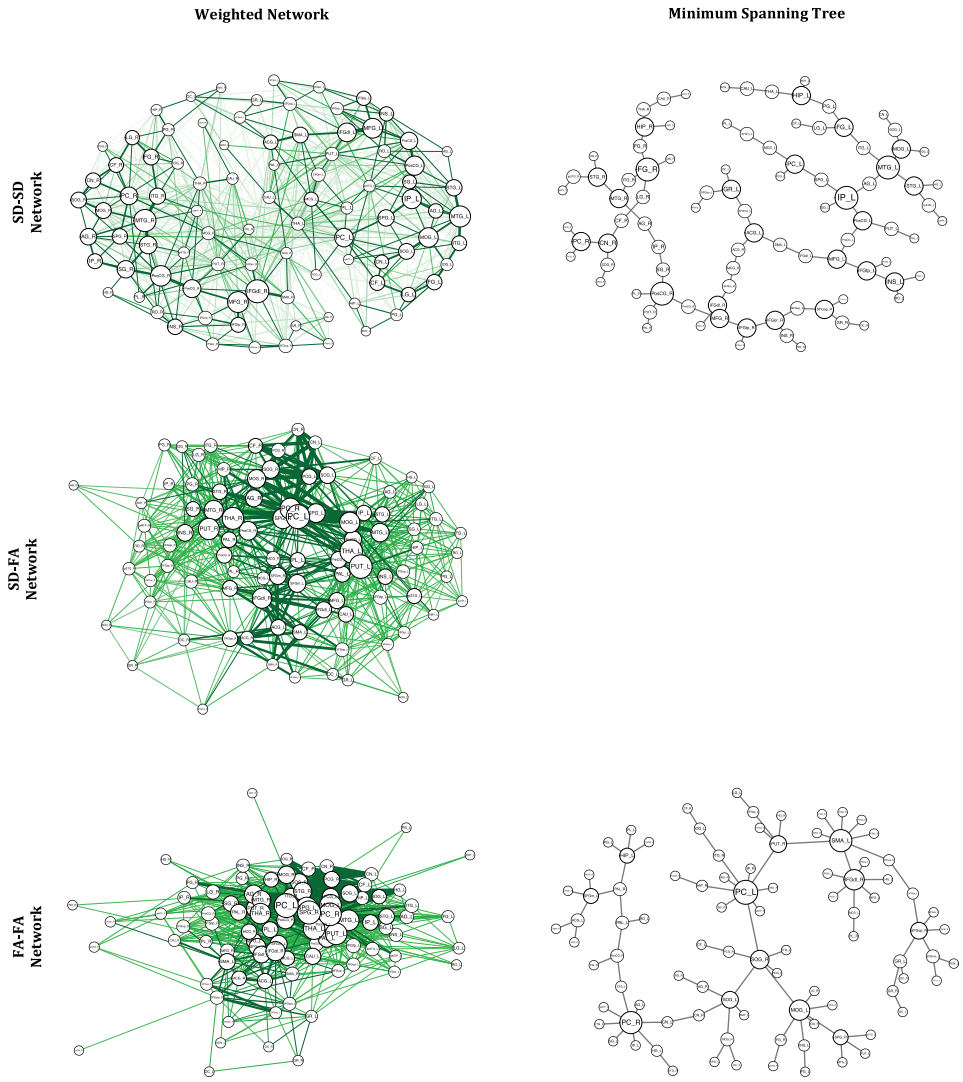

Figure 2. Visual representations of the constructed structural networks

Note. Structural networks based on various definitions of connectivity. We used streamline density (SD) to define connectivity matrices that capture the network with the highest connectivity probability (i.e. the connectivity probability network). These binary SD-defined matrices were subsequently weighted for SD to account for differences in connectivity probability between brain regions (SD-SD matrices), and were also weighted for fractional anisotropy (FA) in order to account for differences in connectivity integrity within the connectivity probability network (SD-FA matrices). We also constructed FA-defined matrices in order to capture the network with the highest connectivity integrity (i.e. the connectivity integrity network), which were weighted for FA to account for differences in connectivity integrity between brain regions in this network (FA-FA matrices). The minimum spanning tree (MST) is a unique binary graph that captures acyclic (i.e. tree-shaped) connections between all ROIs in the network while minimizing the sum of weights (Stam et al., 2014). Calculation of the MST on the SD-FA matrices was omitted since the resulting binary graph would be identical to the MST of the FA-FA matrices. The displayed networks are based on trauma control group averages (weighted networks were thresholded at 20%). FA = fractional anisotropy; SD = streamline density).

Table 3. Comparison of interhemispheric connectivity in the structural networks

	Network Definition			ANOVA	
	SD-SD	SD-FA	FA-FA	*F*	P
Weighted Networks					
Interhemispheric Weight, %					
10% Threshold	3.3 (0.5)	15.2 (1.9)	68.1 (2.0)		
15% Threshold	3.8 (0.5)	21.7 (2.1)	52.6 (0.8)		
20% Threshold	4.0 (0.5)	25.4 (2.0)	42.7 (0.5)		
Network Definition				95448.3[a]	**< .001**
Matrix Threshold				1475.1[a]	**< .001**
Definition * Threshold				10311.9[b]	**< .001**
Minimum Spanning Tree					
Interhemispheric Links, %	2.6 (0.3)	-	79.5 (1.8)		
Network Definition				107858.3[a]	**< .001**

Note. Data reflect mean (standard deviation), unless otherwise indicated. ANOVA = analysis of variance; FA = fractional anisotropy; SD = streamline density.
[a]Degrees of freedom: 2,61. [b]Degrees of freedom: 4,59.

GLOBAL NETWORK PROPERTIES

SD-SD NETWORK

The results of analyses assessing the impact of TBI on global network properties of weighted SD-SD networks (see Figure 3) revealed significant main effects of group on *transitivity* ($F(1,62) = 4.4$, $p = .04$) and *assortativity* ($F(1,62) = 4.4$, $p = .04$), while no significant effects on *characteristic path length* or *modularity* were observed ($Fs(1,62) \leq 1.0$, $ps \geq .32$). Post-hoc group comparisons revealed that the moderate/severe TBI group had higher *transitivity* ($p = .04$, $d = 0.70$) and higher *assortativity* ($p = .04$, $d = 0.70$) as compared to the TC group, while no other group differences were observed ($ps \geq .20$). Analyses investigating the impact of TBI on the MST of the SD-SD network revealed no effects of group on global network parameters ($ps \geq .39$). These findings indicate that moderate/severe TBI increases local clustering (i.e. higher *transitivity*) and hierarchy (i.e. higher *assortativity*) in the connectivity probability network, while no impact of TBI was observed on the structural backbone of this network.

SD-FA NETWORK

The results of analyses on the weighted SD-FA network (Figure 3) revealed a significant main effect of group on *characteristic path length* ($F(1,62) = 5.7$, $p = .02$), while no effects of TBI severity were found on *transitivity, modularity* or *assortativity* ($Fs(1,62) \leq 2.6$, $ps \geq .11$). Post-hoc group comparisons revealed longer *characteristic path length* in the moderate/severe TBI group as compared to the TC group ($p = .02$, $d = 0.79$), while no other significant group differences were observed ($ps \geq .10$). Taken together, these findings indicate

that moderate/severe TBI reduces structural integration in the connectivity probability network when accounting for connectivity integrity.

FA-FA NETWORK

Analyses on the weighted FA-FA networks (Figure 3) also showed a significant main effect of group on *characteristic path length* ($F(1,62) = 5.7$, $p = .02$), while no effects were observed on *transitivity, modularity or assortativity* ($Fs(1,62) \leq 0.6$, $ps \geq .46$). Again, post-hoc group comparisons showed that the moderate/severe TBI group had longer *characteristic path length* ($p = .02$, $d = 0.75$) while no other group differences were observed ($ps \geq .08$). Analyses on the MST of the FA-FA network did not reveal significant main effects of TBI severity on *modularity* or *assortativity* ($Fs(1,62) \leq 1.7$, $ps \geq .18$), while we found a significant main effect of TBI severity on *characteristic path length* ($F(1,62) = 4.4$, $p = .04$). Post-hoc group comparisons revealed that the moderate/severe TBI group had longer *characteristic path length* in the MST of the FA-FA network than the TC group ($p = .04$, $d = 0.66$). Taken together, these findings indicate that moderate/severe TBI decreases structural integration in the connectivity integrity network, which is also reflected by the structural backbone of the connectivity integrity network.

MATRIX THRESHOLD

For network parameters derived from weighted networks with obtained effects of group (*transitivity* and *assortativity* in the weighted SD-SD network and *characteristic path length* in the weighted SD-FA, FA-FA networks), we investigated the influence of matrix threshold on the observed effects of group using the interaction effects between matrix threshold and group. None of these analyses revealed a significant interaction effect ($Fs(2,60) \leq 1.6$, $ps \geq .17$), indicating that the observed effects of group on network parameters did not vary across the assessed matrix thresholds.

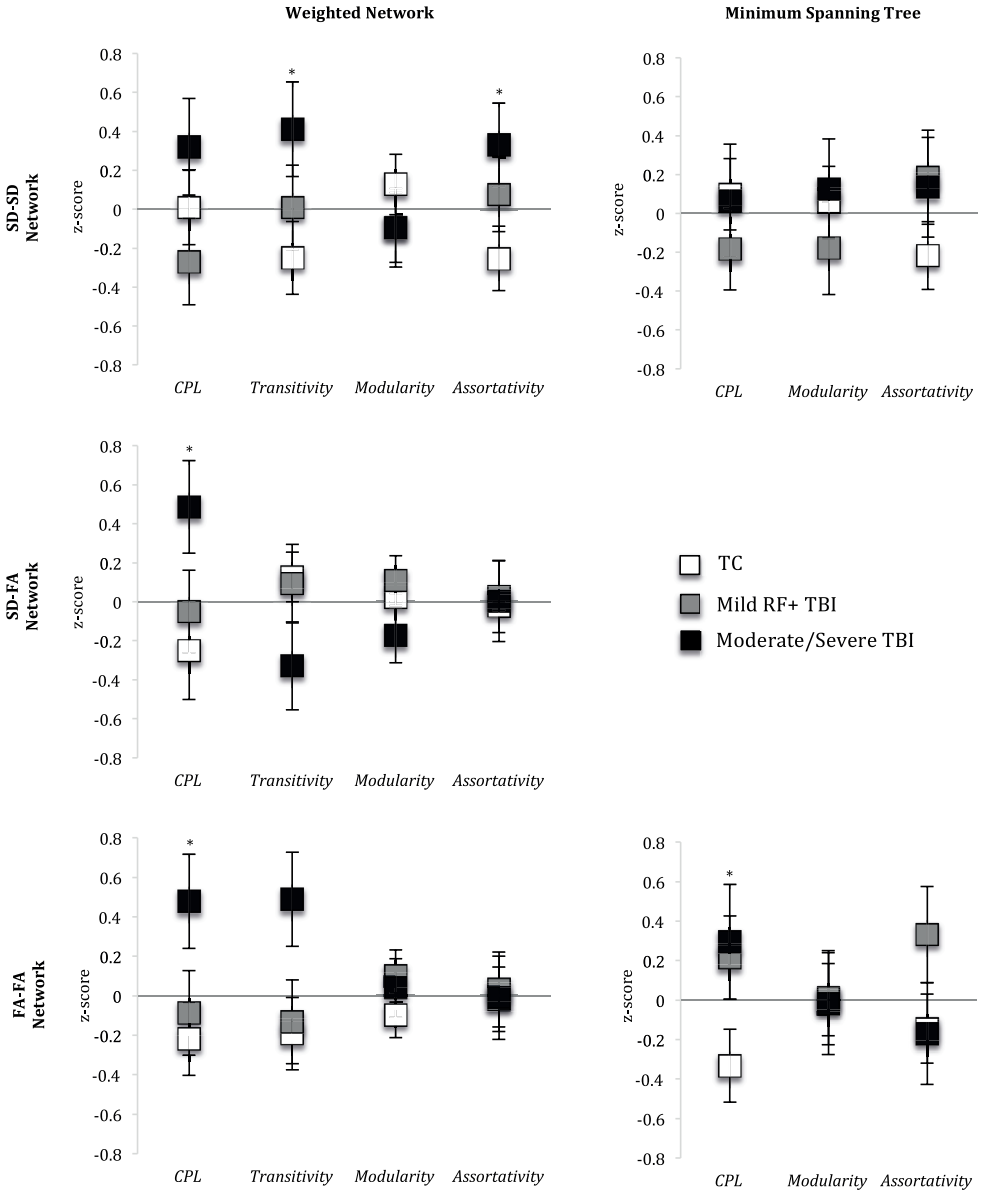

Figure 3. The impact of TBI on global network parameters in the structural connectome

Note. All axes depict z-scores and error bars indicate standard error. Network parameters derived from weighted networks are averaged across matrix thresholds. *Transitivity* was not calculated for the minimum spanning tree, since this is an acyclic network. *CPL = characteristic path length*; FA = fractional anisotropy; RF= risk factor; SD = streamline density; TC = trauma control; TBI = traumatic brain injury.

*$p < .05$. **$p < .01$. ***$p < .001$.

RELATIONS BETWEEN STRUCTURAL CONNECTIVITY AND FUNCTIONAL OUTCOME

First, we assessed the relations among network parameters with obtained effects of TBI (*transitivity* and *assortativity* in the weighted SD-SD network and *characteristic path length* in the weighted SD-FA, FA-FA networks and the MST of the FA-FA network). The results showed that within the SD-SD network, higher *transitivity* was related to higher *assortativity* (r = .42, p = .01). Furthermore, longer *characteristic path length* in the SD-FA network was strongly related to longer *characteristic path length* in the FA-FA network (r = .95, p < .001). No other significant relations were observed (rs ≤.19, ps ≥ .28), suggesting that the impact of moderate/severe TBI on (1) the SD-SD network (higher *transitivity* and *assortativity*); (2) the SD-FA and FA-FA networks (longer *characteristic path length*); and (3) the MST of the FA-FA network (longer *characteristic path* length) may represent relatively independent mechanisms in the neuropathology of TBI.

Second, we assessed the relations between network parameters with obtained effects of TBI and aspects of neurocognitive and behavioral functioning with sensitivity to TBI (FSIQ, working memory, RAVLT encoding and internalizing and externalizing behavior problems). In the sample of children with TBI, longer *characteristic path length* in the weighted SD-FA network was associated with lower FSIQ (r = -0.35, p = .04) and poorer working memory performance (r = -0.44, p = .007). Likewise, longer *characteristic path length* in the weighted FA-FA network was associated with poorer working memory performance (r = -0.42, p = .01). Interestingly, *longer characteristic path length* in the MST of the FA-FA network was related to *better* working memory performance (r = 0.39, p = .02). The significant relations observed in the TBI sample were not replicated in the TC group (rs ≤ .15, ps ≥ .47) and other relations between network parameters and aspects of neurocognitive and behavioral functioning in the TBI sample did not reach conventional levels of significance (rs ≤ .30, ps ≥ .08). Taken together, these findings suggest that the influence of moderate/severe TBI on *characteristic path length* is related to important aspects of neurocognitive outcome (FSIQ and working memory), but not to behavioral functioning after moderate/severe TBI.

THE ROLES OF LINKS, NODES AND WEIGHTS

Since the number of links, number of nodes and total link weight in the network (i.e. sum of all link weights) are known to influence the properties of the assessed weighted networks (Stam et al., 2014), we performed an exploratory analysis to investigate whether group differences in these network components may have influenced the observed effects of moderate/severe TBI on network parameters (for details, see Supporting Information). This analysis revealed that the number of links and nodes did not influence

the observed effects of moderate/severe TBI on global network parameters. In contrast, we found that the moderate/severe TBI group had lower total link weight in the SD-FA and FA-FA networks that could potentially have accounted for the observed effect of moderate/severe TBI on *characteristic path length* after moderate/severe TBI in these networks. Consistent with this idea, very strong correlations between lower total weight and *characteristic path length* were observed in these networks (*r*s ≥ .95). Taken together, these findings suggest that the global detrimental impact of moderate/severe TBI on total FA weight in the structural network directly translates into longer *characteristic path length* in FA weighted networks.

DISCUSSION

This study used probabilistic tractography in combination with graph theory to study the structural connectome in children with mild to severe TBI during the chronic phase of recovery. The results of this study show that network definition and weighting strongly influence the reconstruction of the connectome, in terms of its sensitivity for interhemispheric connectivity as well as the impact of TBI. Analyses concerning the impact of TBI on the structural connectome revealed that children with moderate/severe TBI have abnormal organization of a structural networks defined by SD (i.e. the connectivity probability network) and by FA (i.e. connectivity integrity network). Specific aspects of abnormal structural connectivity were related to decreased neurocognitive functioning in children with TBI (i.e. FSIQ and working memory), while no evidence was found for relations between structural connectivity and behavioral functioning. The results of this study contribute to our understanding of the impact of moderate/severe TBI on the structural connectome and its potential implication in neurocognitive dysfunction after pediatric TBI.

Analyses on network construction showed that the measure of connectivity that is chosen to define and/or weight structural connectivity (e.g. SD or FA) greatly influences the reconstruction of the connectome in terms of its sensitivity for interhemispheric connectivity. More specifically, the connectivity probability (i.e. SD-SD) network predominantly captures intrahemispheric connectivity, while the connectivity integrity (FA-FA) network has higher sensitivity to interhemispheric connectivity. Likewise, accounting for connectivity integrity in the connectivity probability network (i.e. SD-FA network), increased its sensitivity for interhemispheric connectivity. Although it has previously been reported that network definition can influence network properties (Qi et al., 2015), we think this study is the first to show the influence of various network definitions on the sensitivity of structural networks to interhemispheric connectivity.

Analyses aimed at elucidating the impact of pediatric TBI on the structural connectome revealed no evidence for an impact of mild^{RF+} TBI on structural connectivity. This finding is in line with our earlier study that used DTI in combination with tract-based spatial statistics to study white matter integrity, revealing no evidence for reduced white matter integrity in children with mild^{RF+} TBI (Königs et al., submitted). That study did show decreased white matter volume in children with mild^{RF+} TBI, but the current study suggests that this may not translate to abnormal organization of the connectome. The negative findings in children with mild^{RF+} TBI further suggest that the reported effects of mild pediatric TBI on structural connectivity in the acute phase of recovery (Yuan et al.,

2015) may be essentially transient in nature, for example caused by temporary cerebral edema or compensated for by neural plasticity. This hypothesis awaits empirical testing in future research.

In contrast to mild^{RF+} TBI, children with moderate/severe TBI were found to have abnormal organization of the connectivity probability network as well as the connectivity integrity network. When compared to the connectivity probability network of children in the trauma control group, children with moderate/severe TBI had higher *transitivity* and *assortativity* suggesting increased local clustering and increased hierarchy of connectivity probability. The observed sensitivity of the connectivity probability network for intra-hemispheric connections, may suggest that these findings are primarily applicable to intrahemispheric connections. When accounting for connectivity integrity in the connectivity probability network, we also observed increased *characteristic path length* indicative of decreased structural integration. The current findings converge with previous studies reporting increased *characteristic path length* in the connectivity probability network after moderate/severe TBI in adults (Caeyenberghs et al., 2014; Caeyenberghs, Leemans, Heitger, et al., 2012; Kim et al., 2014) and extend these findings by showing that moderate/severe TBI in children also increases structural segregation (i.e. higher *transitivity*) and hierarchy (i.e. higher *assortativity*) of connectivity probability. Use of the minimum spanning tree (i.e. MST) to study the structural backbone of the connectivity probability network revealed no evidence for an impact of moderate/severe TBI.

With regard to the connectivity integrity network, children with moderate/severe TBI were found to have increased *characteristic path length*. This finding indicates that moderate/severe TBI in children impacts structural integration in the connectome in terms of connectivity integrity, which is in line with reports in adults with moderate to severe TBI (Caeyenberghs et al., 2014; Kim et al., 2014). The observed relative sensitivity of the connectivity integrity network for interhemispheric connectivity may suggest that the impact of moderate/severe TBI on *characteristic path length* primarily applies to interhemispheric connections. This idea is consistent with the central role of the corpus callosum in the neuropathology of TBI (Aoki, Inokuchi, Gunshin, Yahagi, & Suwa, 2012). An exploratory analysis investigating the influence of group differences in network components (i.e. the number of nodes and links, and total link weight in the network) revealed that the global detrimental impact of moderate/severe TBI on FA in the directly translates into the observed longer *characteristic path length* in FA-weighted networks (i.e. SD-FA and FA-FA networks). However, analysis on the MST, which is robust to the influence of group differences in total link weight, also revealed increased *characteristic path length* in the backbone of the connectivity integrity network. This finding indicates

that the impact of moderate/severe TBI on *characteristic path length* in the connectivity probability network was not merely accounted for by a global effect of moderate/severe TBI on FA weight on the network.

Analyses investigating the relation between aspects of structural connectivity and functional outcome following pediatric TBI revealed no associations between network measures and behavior problems as observed by parents and teachers. This finding may suggest that behavioral functioning after pediatric TBI is not related to global connectivity, but is rather dependent on more specific (e.g. frontostriatal) subnetworks (Max, Wilde, & Bigler, 2012). With regard to neurocognitive functioning, longer *characteristic path length* was associated with lower intelligence (in the connectivity probability network) and poorer working memory (in both the connectivity probability and the connectivity integrity networks). These findings indicate that globally decreased structural integration in the connectome may be implicated in neurocognitive dysfunction following moderate/severe TBI in children, which is in line with the existing literature (Caeyenberghs et al., 2014; Kim et al., 2014). Interestingly, longer *characteristic path length* in the structural backbone of the connectivity integrity network was related to *better* working memory performance. In line with these findings, *characteristic path length* in the weighted connectivity integrity network was not related to *characteristic path length* in the backbone, the MST, of that same network. Together, these counter-intuitive findings suggest that the observed increased *characteristic path length* in the backbone of the connectivity integrity network may actually reflect an adaptive plasticity response to the impact of moderate/severe TBI, attempting to reconnect the disintegrated network by reorganizing its structural backbone (with high integrity connections) in a more distributed fashion**.** This hypothesis requires empirical testing in future longitudinal studies into post-injury development of the connectome in children with moderate/severe TBI.

This study had some weaknesses. First, we investigated a relatively small sample of patients (n = 63), especially with regard to the moderate/severe TBI group (n = 16). Therefore, negative findings in this study may be the result of limited statistical power. Second, a limited set of instruments was used to measure outcome in terms of neurocognitive and behavioral functioning. Third, the moderate/severe TBI group had lower SES than the TC group, which potentially could have confounded the observed impact of moderate/severe TBI on structural connectivity. However, exploratory analysis revealed that SES was unlikely to have confounded the observed effects of moderate/severe TBI, since SES was not significantly associated with the relevant network measures in the trauma control group (rs ≤ .20 ps ≥ .32). Strong points of this study include: (1) the use of a trauma control group to account for premorbid risk factors that may increase the risk of TBI

(e.g. psychiatric disorder); (2) the use of various measures of connectivity to define and weight the structural network in order to capture differential aspects of the structural connectome (i.e. the connectivity probability and connectivity integrity networks), with differential sensitivity for interhemispheric connectivity; (3) and the use of the MST to selectively investigate connectivity in the structural backbone of the connectome.

In conclusion, this is the first study investigating the structural connectome of children with mild to severe TBI in the chronic phase of recovery. The results show that children with moderate/severe TBI have aberrant organization of the connectome, which further relates to outcomes in terms of post-injury neurocognitive functioning. More specifically, children with moderate/severe TBI had increased local clustering and hierarchy in a network of high probability connections and reduced structural integration in a network of high integrity connections. Measures of structural integration were related to intelligence and working memory, suggesting that this aspect of structural connectivity may be implicated in neurocognitive dysfunction after pediatric TBI.

REFERENCES

American College of Surgeons. (2004). *Advanced Trauma Life Support Program for Doctors*. (Committee on Trauma, Ed.) (7th ed.).

Aoki, Y., Inokuchi, R., Gunshin, M., Yahagi, N., & Suwa, H. (2012). Diffusion tensor imaging studies of mild traumatic brain injury: a meta-analysis. *Journal of Neurology, Neurosurgery, and Psychiatry*, *83*(9), 870–6. doi:10.1136/jnnp-2012-302742

Babcock, L., Yuan, W., Leach, J., Nash, T., & Wade, S. (2015). White matter alterations in youth with acute mild traumatic brain injury. *Journal of Pediatric Rehabilitation Medicine*, *8*(4), 285–96. doi:10.3233/PRM-150347

Babikian, T., & Asarnow, R. (2009). Neurocognitive outcomes and recovery after pediatric TBI: meta-analytic review of the literature. *Neuropsychology*, *23*(3), 283–296. doi:10.1037/a0015268

Behrens, T. E. J., Woolrich, M. W., Jenkinson, M., Johansen-Berg, H., Nunes, R. G., Clare, S., … Smith, S. M. (2003). Characterization and propagation of uncertainty in diffusion-weighted MR imaging. *Magnetic Resonance in Medicine : Official Journal of the Society of Magnetic Resonance in Medicine / Society of Magnetic Resonance in Medicine*, *50*(5), 1077–88. doi:10.1002/mrm.10609

Caeyenberghs, K., Leemans, A., De Decker, C., Heitger, M., Drijkoningen, D., Linden, C. Vander, … Swinnen, S. P. (2012). Brain connectivity and postural control in young traumatic brain injury patients: A diffusion MRI based network analysis. *NeuroImage. Clinical*, *1*(1), 106–15. doi:10.1016/j.nicl.2012.09.011

Caeyenberghs, K., Leemans, A., Heitger, M. H., Leunissen, I., Dhollander, T., Sunaert, S., … Swinnen, S. P. (2012). Graph analysis of functional brain networks for cognitive control of action in traumatic brain injury. *Brain : A Journal of Neurology*, *135*(Pt 4), 1293–307. doi:10.1093/brain/aws048

Caeyenberghs, K., Leemans, A., Leunissen, I., Gooijers, J., Michiels, K., Sunaert, S., & Swinnen, S. P. (2014). Altered structural networks and executive deficits in traumatic brain injury patients. *Brain Structure & Function*, *219*(1), 193–209. doi:10.1007/s00429-012-0494-2

Cohen, J. (1988). *Statistical power analysis for the behavioral science*. Hillsdale, NY: Erlbaum.

Dall'Acqua, P., Johannes, S., Mica, L., Simmen, H.-P., Glaab, R., Fandino, J., … Hänggi, J. (2016). Connectomic and Surface-Based Morphometric Correlates of Acute Mild Traumatic Brain Injury. *Frontiers in Human Neuroscience*, *10*, 127. doi:10.3389/fnhum.2016.00127

Epskamp, S., Cramer, A. O. J., Waldorp, L. J., Schmittmann, V. D., & Borsboom, D. (2012). qgraph : Network Visualizations of Relationships in Psychometric Data. *Journal of Statistical Software*, *48*(4), 1–18. doi:10.18637/jss.v048.i04

Fagerholm, E. D., Hellyer, P. J., Scott, G., Leech, R., & Sharp, D. J. (2015). Disconnection of network hubs and cognitive impairment after traumatic brain injury. *Brain : A Journal of Neurology*, *138*(Pt 6), 1696–709. doi:10.1093/brain/awv075

Gong, G., He, Y., Concha, L., Lebel, C., Gross, D. W., Evans, A. C., & Beaulieu, C. (2009). Mapping anatomical connectivity patterns of human cerebral cortex using in vivo diffusion tensor imaging tractography. *Cerebral Cortex (New York, N.Y. : 1991)*, *19*(3), 524–36. doi:10.1093/cercor/bhn102

Jenkinson, M., Beckmann, C. F., Behrens, T. E. J., Woolrich, M. W., & Smith, S. M. (2012). FSL. *NeuroImage*, *62*(2), 782–90. doi:10.1016/j.neuroimage.2011.09.015

Kim, J., Parker, D., Whyte, J., Hart, T., Pluta, J., Ingalhalikar, M., … Verma, R. (2014). Disrupted structural connectome is associated with both psychometric and real-world neuropsychological impairment in diffuse traumatic brain injury. *Journal of the International Neuropsychological Society : JINS*, *20*(9), 887–96. doi:10.1017/S1355617714000812

Königs, M., Heij, H. A., van der Sluijs, J. A., Vermeulen, R. J., Goslings, J. C., Luitse, J. S. K., … Oosterlaan, J. (2015). Pediatric Traumatic Brain Injury and Attention Deficit. *Pediatrics*, *136*(3), 534–541. doi:10.1542/peds.2015-0437

Königs, M., Pouwels, P. J. W., van Heurn, L. W. E., Vermeulen, R. J., Goslings, J. C., Poll-The, B. T., … Oosterlaan, J. (n.d.). Neurocognitive and Behavioral Impairment after Pediatric Traumatic Brain Injury. *Submitted*.

Lehmann, E., & D'Abrera, H. (2006). *Nonparametrics: statistical methods based on ranks*. New York: Springer.

Li, L., & Liu, J. (2013). The effect of pediatric traumatic brain injury on behavioral outcomes: a systematic review. *Developmental Medicine and Child Neurology*, *55*(1), 37–45. doi:10.1111/j.1469-8749.2012.04414.x

Max, J., Koele, S., & Smith Jr., W. (1998). Psychiatric disorders in children and adolescents after severe traumatic brain injury: a controlled study. *Child & Adolescent Psychiatry*, *37*(8), 932–840.

Max, J., Wilde, E., & Bigler, E. (2012). Neuroimaging correlates of novel psychiatric disorders after pediatric traumatic brain injury. *Child & Adolescent Psychiatry*, *51*(11), 1208–1217.

Otte, W. M., van Diessen, E., Paul, S., Ramaswamy, R., Subramanyam Rallabandi, V. P., Stam, C. J., & Roy, P. K. (2015). Aging alterations in whole-brain networks during adulthood mapped with the minimum spanning tree indices: The interplay of density, connectivity cost and life-time trajectory. *NeuroImage*, *109*, 171–189. doi:10.1016/j.neuroimage.2015.01.011

Park, H., & Friston, K. (2013). Structural and functional brain networks: from connections to cognition. *Science*, *342*(6158), 579–587.

Patenaude, B., Smith, S. M., Kennedy, D. N., & Jenkinson, M. (2011). A Bayesian model of shape and appearance for subcortical brain segmentation. *NeuroImage*, *56*(3), 907–922. doi:10.1016/j.neuroimage.2011.02.046

Qi, S., Meesters, S., Nicolay, K., Romeny, B. M., & Ossenblok, P. (2015). The influence of construction methodology on structural brain network measures: a review. *Journal of Neuroscience Methods*, *253*, 170–182. doi:10.1016/j.jneumeth.2015.06.016

Roberts, R., Mathias, J., & Rose, S. (2014). Diffusion Tensor Imaging (DTI) Findings Following Pediatric Non-Penetrating TBI: A Meta-Analysis. *Developmental Neuropsychology*, *39*(8), 600–637.

Rubinov, M., & Sporns, O. (2010). Complex network measures of brain connectivity: Uses and interpretations. *NeuroImage*, *52*(3), 1059–1069. doi:10.1016/j.neuroimage.2009.10.003

Sattler, J. M. (2001). Assessment of children: cognitive applications. Jerome M. *Sattler, San Diego*, 774.

Sharp, D. J., Scott, G., & Leech, R. (2014). Network dysfunction after traumatic brain injury. *Nature Reviews. Neurology*, *10*(3), 156–66. doi:10.1038/nrneurol.2014.15

Squarcina, L., Bertoldo, A., Ham, T. E., Heckemann, R., & Sharp, D. J. (2012). A robust method for investigating thalamic white matter tracts after traumatic brain injury. *NeuroImage*, *63*(2), 779–788. doi:10.1016/j.neuroimage.2012.07.016

Stam, C. J. (2014). Modern network science of neurological disorders. *Nature Reviews Neuroscience*, *15*(10), 683–695. doi:10.1038/nrn3801

Stam, C. J., Tewarie, P., Van Dellen, E., van Straaten, E. C. W., Hillebrand, A., & Van Mieghem, P. (2014). The trees and the forest: Characterization of complex brain networks with minimum spanning trees. *International Journal of Psychophysiology : Official Journal of the International Organization of Psychophysiology*, *92*(3), 129–38. doi:10.1016/j.ijpsycho.2014.04.001

Statistics Netherlands. (2006). *Education Categorization Standard [Standaard onderwijsindeling 2006]*. *www.cbs.nl*.

Teasdale, G., & Jennett, B. (1976). Assessment and prognosis of coma after head injury. *Acta Neurochirurgica*, *34*(1-4), 45–55.

Van Beek, L., Vanderauwera, J., Ghesquiere, P., Lagae, L., & De Smedt, B. (2015). Longitudinal changes in mathematical abilities and white matter following paediatric mild traumatic brain injury. *Brain Injury*, *9052*(November), 1–10. doi:10.3109/02699052.2015.1075172

van den Burg, W., & Kingma, a. (1999). Performance of 225 Dutch school children on Rey's Auditory Verbal Learning Test (AVLT): parallel test-retest reliabilities with an interval of 3 months and normative data. *Archives of Clinical Neuropsychology : The Official Journal of the National Academy of Neuropsychologists*, *14*(6), 545–59

Verhulst, F., & van der Ende, J. (2013). *Handeling ASEBA Vragenlijsten voor leeftijden 6 t/m 18 jaar: CBCL/6-18, YSR & TRF*. ASEBA.

Vos, P., & Battistin, L. (2002). EFNS guideline on mild traumatic brain injury: report of an EFNS task force. *European Journal of Neurology*, *9*(3), 207–219. Retrieved from http://onlinelibrary.wiley.com/doi/10.1046/j.1468-1331.2002.00407.x/full

Vu, J. A., Babikian, T., & Asarnow, R. F. (2011). Academic and Language outcomes in Children after Traumatic Brain Injury A Meta Analysis. *Exceptional Children*, *77*(3), 263–281.

Wechsler, D. (2005). *WISC–IIINL: Wechsler Intelligence Scale for Children. Derde editie NL. Handleiding en Verantwoording*. *The Psychological Corporation*. London: Hartcourt Assessment.

World Health Organization. (2006). *Neurological disorders: public health challenges*. World Health Organization

Yuan, W., Wade, S. L., & Babcock, L. (2015). Structural connectivity abnormality in children with acute mild traumatic brain injury using graph theoretical analysis. *Human Brain Mapping*, *36*(2), 779–92. doi:10.1002/hbm.22664

Zhang, Y., Brady, M., & Smith, S. (2001). Segmentation of brain MR images through a hidden Markov random field model and the expectation-maximization algorithm. *IEEE Transactions on Medical Imaging*, *20*(1), 45–57. doi:10.1109/42.906424

SUPPORTING INFORMATION

NETWORK NODES

Table S1. Abbreviations of Network Nodes

Abbreviation	Network Node	Hemisphere	Origin
GR_L	Gyrus Rectus	Left	AAL
OC_L	Olfactory Cortex	Left	AAL
SFGop_L	Superior frontal gyrus orbital part	Left	AAL
SFGmo_L	Superior frontal gyrus medial orbital	Left	AAL
MFGop_L	Middle frontal gyrus orbital part	Left	AAL
IFGor_L	Inferior frontal gyrus orbital part	Left	AAL
IFGdl_L	Superior frontal gyrus dorsolateral	Left	AAL
MFG_L	Middle frontal gyrus	Left	AAL
IFGop_L	Inferior frontal gyrus opercular part	Left	AAL
IFGtp_L	Inferior frontal gyrus triangular part	Left	AAL
SMA_L	Supplementary motor area	Left	AAL
SFGm_L	Superior frontal gyrus medial	Left	AAL
PL_L	Paracentral lobule	Left	AAL
PreCG_L	Precentral gyrus	Left	AAL
RO_L	Rolandic operculum	Left	AAL
PosCG_L	Postcentral gyrus	Left	AAL
SPG_L	Superior parietal gyrus	Left	AAL
IP_L	Inferior parietal but supramarginal and angular gyri	Left	AAL
SG_L	Supramarginal gyrus	Left	AAL
AG_L	Angular gyrus	Left	AAL
PC_L	Precuneus	Left	AAL
SOG_L	Superior occipital gyrus	Left	AAL
MOG_L	Middle occipital gyrus	Left	AAL
IOG_L	Inferior occipital gyrus	Left	AAL
CF_L	Calcarine fissure and surrounding cortex	Left	AAL
CN_L	Cuneus	Left	AAL
LG_L	Lingual gyrus	Left	AAL
FG_L	Fusiform gyrus	Left	AAL
HG_L	Heschl gyrus	Left	AAL
STG_L	Superior temporal gyrus	Left	AAL
MTG_L	Middle temporal gyrus	Left	AAL
ITG_L	Inferior temporal gyrus	Left	AAL
tpSTG_L	Temporal pole: superior temporal gyrus	Left	AAL
tpMTP_L	Temporal pole: middle temporal gyrus	Left	AAL
PG_L	Parahippocampal gyrus	Left	AAL
ACG_L	Anterior cingulated and paracingulate gyri	Left	AAL
MCG_L	Median cingulated and paracingulate gyri	Left	AAL
PCG_L	Posterior cingulate gyrus	Left	AAL
INS_L	Insula	Left	AAL
GR_R	Gyrus Rectus	Right	AAL
OC_R	Olfactory Cortex	Right	AAL
SFGop_R	Superior frontal gyrus orbital part	Right	AAL
SFGmo_R	Superior frontal gyrus medial orbital	Right	AAL
MFGop_R	Middle frontal gyrus orbital part	Right	AAL

Abbreviation	Network Node	Hemisphere	Origin
IFGor_R	Inferior frontal gyrus orbital part	Right	AAL
IFGdl_R	Superior frontal gyrus dorsolateral	Right	AAL
MFG_R	Middle frontal gyrus	Right	AAL
IFGop_R	Inferior frontal gyrus opercular part	Right	AAL
IFGtp_R	Inferior frontal gyrus triangular part	Right	AAL
SMA_R	Supplementary motor area	Right	AAL
SFGm_R	Superior frontal gyrus medial	Right	AAL
PL_R	Paracentral lobule	Right	AAL
PreCG_R	Precentral gyrus	Right	AAL
RO_R	Rolandic operculum	Right	AAL
PosCG_R	Postcentral gyrus	Right	AAL
SPG_R	Superior parietal gyrus	Right	AAL
IP_R	Inferior parietal but supramarginal and angular gyri	Right	AAL
SG_R	Supramarginal gyrus	Right	AAL
AG_R	Angular gyrus	Right	AAL
PC_R	Precuneus	Right	AAL
SOG_R	Superior occipital gyrus	Right	AAL
MOG_R	Middle occipital gyrus	Right	AAL
IOG_R	Inferior occipital gyrus	Right	AAL
CF_R	Calcarine fissure and surrounding cortex	Right	AAL
CN_R	Cuneus	Right	AAL
LG_R	Lingual gyrus	Right	AAL
FG_R	Fusiform gyrus	Right	AAL
HG_R	Heschl gyrus	Right	AAL
STG_R	Superior temporal gyrus	Right	AAL
MTG_R	Middle temporal gyrus	Right	AAL
ITG_R	Inferior temporal gyrus	Right	AAL
tpSTG_R	Temporal pole: superior temporal gyrus	Right	AAL
tpMTP_R	Temporal pole: middle temporal gyrus	Right	AAL
PG_R	Parahippocampal gyrus	Right	AAL
ACG_R	Anterior cingulated and paracingulate gyri	Right	AAL
MCG_R	Median cingulated and paracingulate gyri	Right	AAL
PCG_R	Posterior cingulate gyrus	Right	AAL
INS_R	Insula	Right	AAL
THA_L	Thalamus	Left	FIRST
CAU_L	Caudate	Left	FIRST
PUT_L	Putamen	Left	FIRST
PAL_L	Pallidum	Left	FIRST
HIP_L	Hippocampus	Left	FIRST
AMY_L	Amygdala	Left	FIRST
ACN_L	Accumbens	Left	FIRST
THA_R	Thalamus	Right	FIRST
CAU_R	Caudate	Right	FIRST
PUT_R	Putamen	Right	FIRST
PAL_R	Pallidum	Right	FIRST
HIP_R	Hippocampus	Right	FIRST
AMY_R	Amygdala	Right	FIRST
ACN_R	Accumbens	Right	FIRST

Note. AAL = Automated Anatomical Atlas (Gong et al., 2009). FIRST (Patenaude et al., 2011) refers to a model-based segmentation tool from the Functional MRI of the Brain Software Library (FSL).

FUNCTIONAL OUTCOME

In a previous study (Königs et al.) we found that children with mild^{RF+} TBI and children with moderate/severe TBI had decreased neurocognitive functioning and increased behavior problems (see Table S2 below). In short, the mild^{RF+} TBI and moderate/severe TBI group had lower FSIQ (p = .003, d = -0.93 and p = .02, d = -0.84), poorer working memory performance (p = .005, d = -0.92 and p = 0.04, d = -0.67) and poorer encoding in long-term verbal memory (p = .04 , d = -0.63 and p = .01, d = -0.86) than the TC group. With regard to behavioral functioning, the mild^{RF+} TBI and moderate/severe TBI groups had higher ratings of internalizing problems than the TC group (p = .02, d = 0.85 and p = .005, d = 0.88) and the mild^{RF+} TBI group had higher ratings of externalizing problems as compared to the TC group (p = .001, d = 1.13).

Table S2 . Group comparison on aspects of functional outcome

	Group			ANOVA		
	TC	Mild RF^{+} TBI	Moderate/Severe TBI	$F(2,60)$	p	Contrasts
n	27	20	16			
Neurocognitive functioning						
FSIQ	0.47 (0.82)	-0.37 (1.04)	-0.24 (0.93)	5.6	**.006**	M, MS < TC
Digit Span	0.44 (0.87)	-0.36 (0.91)	-0.17 (1.01)	4.0	**.01**	M, MS < TC
RAVLT Encoding	0.40 (0.90)	-0.20 (1.05)	-0.37 (0.95)	3.9	**.03**	M, MS < TC
Behavior Problems						
Internalizing Problems	-0.44 (0.77)	0.20 (0.77)	0.43 (1.33)	5.1	**.009**	M, MS > TC
Externalizing Problems	-0.37 (0.88)	0.58 (0.84)	-0.14 (1.10)	6.3	**.003**	M > TC, MS

Note. Z scores are reported. Data reflect mean (standard deviation), unless otherwise indicated. FSIQ = full-scale IQ; M = mildRF+ TBI group; MS = moderate/severe TBI group; RAVLT = Rey Auditory Verbal Learning Test; RF = risk factor; TBI = traumatic brain injury; TC = traumatic control.

THE ROLES OF LINKS, NODES AND WEIGHTS

Since the number of links, number of nodes and total link weight in the network (i.e. sum of all link weights) are known to influence the properties of the assessed weighted networks (Stam et al., 2014), we performed an exploratory analyses to investigate whether group differences in these network components may have influenced the observed effects of moderate/severe TBI on network parameters. Since we proportionally thresholded the weighted networks in this study, the number of links was fixed across subjects and could therefore not account for group differences on network parameters. The number of nodes in the weighted networks was not fixed, but did not differ between the moderate/severe TBI and the TC groups (see Table S3) and was therefore unlikely to account for the observed group differences on network parameters.

We also determined the total weight in the weighted networks for each subject and compared these between the TC group and moderate/severe TBI group (Table S3). These group comparisons revealed no significant difference on the total weight in the SD-SD network while the moderate/severe TBI group had lower weight in both the SD-FA network and the FA-FA network. Subsequent exploratory analysis further revealed that total weight in the SD-FA and FA-FA networks was very strongly related to *characteristic path length* in both the SD-FA network (r = -.97, p < .001 and r = -.95, p < .001) and FA-FA network (r = -.94, p < .001 and r = -.99, p < .001). The strength of these correlations suggests that the global detrimental impact of moderate/severe TBI on total FA weight in the structural network directly translates into longer *characteristic path length* in FA weighted networks.

Table S3. Links, nodes and weights in the TC and moderate/severe TBI groups

Network Components[a]	Group		Contrast	
	TC	Moderate/Severe TBI	*p*	Cohen's *d*
n				
Nodes, n				
SD-SD Network	92 (-)	92 (-)	-	-
SD-FA Network	92 (-)	92 (-)	-	-
FA-FA Network	89.1 (0.6)	88.8 (0.6)	.21	-0.49
Total Weight				
SD-SD Network, SD *10^5	342.5 (29.6)	326.9 (29.6)	.10	-0.53
SD-FA Network, FA	279.1 (13.5)	267.8 (13.6)	**.01**	-0.87
FA-FA Network, FA	350.4 (13.5)	339.1 (13.6)	**.01**	-0.85

Note. Data reflect mean (standard deviation), unless otherwise indicated. FA = fractional anisotropy; SD = streamline density; TBI = traumatic brain injury; TC = trauma control.

[a]Displayed values are averaged across matrix thresholds.